Research
A SCIENCE PARTNER JOURNAL

RESEARCH ARTICLE

Lifestyle and Transcriptional Signatures Associated with Ethnicity/Race-Related Variations in the Functional Connectome

Ziteng Han[1], Kexin Wang[1], Tiantian Liu[1*], Fanghui Zhao[1], Yunxiao Ma[2], Wenrui Li[3], Guoyuan Yang[1,4*], and Tianyi Yan[1*]

[1]School of Medical Technology, Beijing Institute of Technology, Beijing, China. [2]School of Life Science, Beijing Institute of Technology, Beijing, China. [3]Department of Biological Sciences, Vanderbilt University, Nashville, TN, USA. [4]School of Interdisciplinary Science, Beijing Institute of Technology, Beijing, China.

*Address correspondence to: tiantian2bit@bit.edu.cn (T.L.); yanggy@bit.edu.cn (G.Y.); yantianyi@bit.edu.cn (T.Y.)

Citation: Han Z, Wang K, Liu T, Zhao F, Ma Y, Li W, Yang G, Yan T. Lifestyle and Transcriptional Signatures Associated with Ethnicity/Race-Related Variations in the Functional Connectome. *Research* 2026;9:Article 1143. https://doi.org/10.34133/research.1143

Submitted 13 September 2025
Revised 20 January 2026
Accepted 22 January 2026
Published 24 March 2026

Copyright © 2026 Ziteng Han et al. Exclusive licensee Science and Technology Review Publishing House. No claim to original U.S. Government Works. Distributed under a Creative Commons Attribution License (CC BY 4.0).

Understanding the variation of functional architecture across individuals and populations is fundamental to advancing our knowledge of human health and behavior. Yet, while functional organization differences related to ethnicity/race are consistently reported, their underlying mechanisms remain poorly understood. Here, we apply precision individualized functional mapping to systematically investigate ethnicity/race-related differences between African American (AA) and white American (WA) cohorts in the brain's intrinsic organization and their associations with lifestyle and transcriptional signatures. We show that variations in network topography and functional connectivity across these ethnic/racial groups follow a hierarchical sensorimotor–association axis and are constrained by brain morphology. Importantly, we identify lifestyle factors—particularly education and substance use—that significantly mediate these associations between ethnicity/race and functional connectivity. Leveraging human brain gene expression data, we further demonstrate that cortical transcriptional patterns are spatially aligned with ethnicity/race-related variability in functional connectivity. Gene ontology analyses of associated genes reveal significant enrichment in biological processes such as synaptic signaling and neuronal system development. Together, these findings uncover a multi-layered framework linking ethnicity/race-related differences in brain function to structural constraints, lifestyle influences, and molecular signatures, and point to the need for a more comprehensive and equitable understanding of human brain diversity.

Introduction

As neuroscience strives for greater generalizability, applicability, and equity, increasing attention has turned to ethnicity/race-related differences in brain structure and function [1,2]. These differences are intertwined with variations in human behaviors and psychiatric outcomes [3,4]. Neuroimaging evidence has consistently shown that anatomical properties such as cortical thickness [5], curvature [6], and gray matter volume [7,8] vary significantly across ethnic/racial populations. Beyond structural aspects, differences have also been observed in intrinsic cortical activity [9] and connectivity profiles [10,11]. Precision mapping techniques reveal that ethnicity/race-related variability in functional network topography is heterogeneously distributed across the cortical mantle [11], aligning with fundamental properties of brain [12]. Yet, given the complex interplay and decoupling of brain structure and function [13,14], studies directly examining the associations between trans-population differences in brain structure and function are lacking. Furthermore, previous structural studies have largely focused on isolated morphological features, potentially overlooking the interregional correlations and coordinated patterns of cortical cytoarchitecture. Morphometric similarity networks (MSNs) offer a solution by integrating multiple morphological features to map the individual-specific anatomical connectome [15]. Therefore, the extent to which ethnicity/race-related differences in the intrinsic functional organization can be explained by this comprehensive structural architecture remains to be systematically investigated.

Ethnicity/race is a social construct embedded within cultural, environmental, and genetic contexts [16]. Focusing narrowly on superficial group differences may risks oversimplification, potential bias, and inequitable treatment of specific populations. Instead, a deeper understanding requires identifying the causes of ethnicity/race-related differences [3,5,17,18]. Prior studies have shown that socioeconomic status strongly influences ethnicity/race differences in health outcomes (e.g., mortality) and treatment-seeking behaviors [19–21], and significantly impacts the development of brain structures [22] and neurocognitive abilities [23]. Moreover, exposure to social stressors and negative experiences can contribute to ethnicity/race-related variability

in neurology and psychopathology (e.g., aging and threat response) [5,24,25]. Recent epidemiological evidence highlights that unhealthy behavioral factors, such as alcohol dependence and lack of physical activity, pose additional risks for both mental and physical health [26,27], and can explain ethnicity/race-related health inequities [17]. Nevertheless, it remains poorly understood whether and how comprehensive lifestyle mediates brain functional variability across populations, a gap that hinders our understanding of the origins of ethnicity/race-related variations in human brain organization.

Furthermore, genetic factors play important roles in brain structure and function [28,29], raising the possibility that patterns of ethnicity/race-related differences in brain functional organization are associated with transcriptional signatures. The Allen Human Brain Atlas (AHBA), which provides a brain-wide map of transcriptional activity across thousands of genes, has been instrumental in linking gene expression to neurodevelopment [30], cortical hierarchy [31], and psychiatric conditions [32,33]. These findings provide valuable insights into the microscale mechanisms that underlie functional connectomes relevant to inter-individual variability and population diversity. More recently, advancements in RNA sequencing from postmortem brain tissues have offered new avenues to uncover the molecular correlates of ethnicity/race-related variability in brain organization. Such studies have shown that genetic ancestry influences gene expression in the brain, with both genetic variations and environments contributing to ancestry-associated expression alterations [34]. Ancestry-associated differentially expressed genes (DEGs) are primarily enriched in immune-related pathways [34,35] and linked to the heritability of neurological disorders [34], echoing the observed prevalence differences across populations [36–38]. Yet, despite these advances, the specific transcriptomic mechanisms underlying ethnicity/race-related variability in brain functional organization remain largely unexplored.

To address these gaps, our study investigates the mechanisms underlying ethnicity/race effects on brain functional connectome from the perspectives of anatomical constraints, lifestyle and environments, and transcription. We leveraged multimodal datasets from the Human Connectome Project (HCP), including the HCP-Young Adult (HCP-YA) and HCP-Development (HCP-D) cohorts, focusing on self-identified African American (AA) and white American (WA) participants. Specifically, we first utilized the advanced multisession hierarchical Bayesian model (MS-HBM) to delineate the individual-specific functional topography and functional connectome architecture. We then used brain-based predictive modeling and linear regression to demonstrate that ethnicity/race is associated with inter-individual variability in resting-state functional connectivity (RSFC) and brain morphological networks. Second, we revealed shared predictive network features across ethnicity/race and various lifestyle variables. We also demonstrated that the functional connectivity correlates of ethnicity/race are partially mediated by lifestyle factors. Finally, by aligning gene expression patterns with functional connectivity features, we revealed transcriptional mechanisms underlying ethnicity/race variations in brain functional organization. Taken together, our work adheres to the latest theoretical framework for neuroimaging research related to ethnicity/race [16] and provides an integrative framework for understanding how structural, lifestyle, and molecular factors converge to shape population-level variability in brain function.

Results

We employed 2 independent large-scale datasets, the HCP-YA and HCP-D datasets, and focused on AA and WA participants. Quality control process followed a previous study [39], and detailed information was provided in Supplementary Methods. Afterward, 101 AA participants and 721 WA participants from the HCP-YA dataset ($N = 822$; age, 22 to 37 years; 435 females) and 68 AA participants and 404 WA participants from the HCP-D dataset ($N = 472$; age, 6 to 21 years; 253 females) were included for subsequent analyses (Table S1). Ethnic/racial groups were categorized based on self-reported information.

Ethnicity/race-related variability in brain functional topography and connectome

The gradient-infused MS-HBM (gMS-HBM), which has been shown to capture the functional organization of individuals precisely, was adopted to generate individual-specific cortical parcellations [40]. In the gMS-HBM framework, each cortical region is assumed to exhibit a unique RSFC pattern, and a unified statistical framework is established, which accounts for inter-individual RSFC variability, intra-individual RSFC variability, and spatial constraints (i.e., encouraging adjacent brain locations with slight changes in RSFC to be assigned the same label) to delineate individualized boundaries under the guidance of group-level parcellation (Schaefer400) [41]. While previous research has characterized individual variability at the level of network topology [42,43], the gMS-HBM offers a deeper level of insight by identifying the fundamental functional units that form these networks within each individual. Resting-state functional magnetic resonance imaging (rs-fMRI) data from all valid sessions of each participant were entered as inputs of gMS-HBM.

To investigate group-level differences in functional topography, we randomly selected 40 AA and 40 WA demographically matched individuals. Using their individual-level parcellations derived from the gMS-HBM, we obtained group-level 400-region parcellation maps (i.e., AA400 and WA400) via a maximum probability fusion approach [44] (Fig. S1). Similarity analyses, quantified with the Dice coefficient, revealed that parcellation maps from the same ethnicity/race group across different datasets exhibited the highest similarity (Fig. S1; e.g., AA400 from the HCP-YA dataset compared with AA400 from the HCP-D dataset: 0.844). By contrast, parcellation maps spanning both datasets and ethnicity/race groups exhibited the greatest spatial distinctions (e.g., AA400 from the HCP-YA dataset compared with WA400 from the HCP-D dataset: 0.784). We then assessed the influence of ethnicity/race on individual-level functional topography. Specifically, the similarity of individual-specific parcellation maps between all AA–WA pairs (101×721 in the HCP-YA dataset and 68×404 in the HCP-D dataset) was calculated and averaged. We observed a nonuniform distribution of variability along the cortex, with the greatest variability in heteromodal association cortices (Fig. 1A and Fig. S1; e.g., control and dorsal attention networks) and the highest similarity in unimodal sensorimotor cortices (especially in the somatomotor and auditory networks).

The individualized parcellations and group-level Schaefer400 parcellations were then applied to rs-fMRI data to generate RSFC matrices (400×400) for each participant separately. For each dataset, AA participants were randomly split into 5 folds, with family structure accounted for, and Hungarian matching was employed to select AA–WA pairs matched on age, sex, and

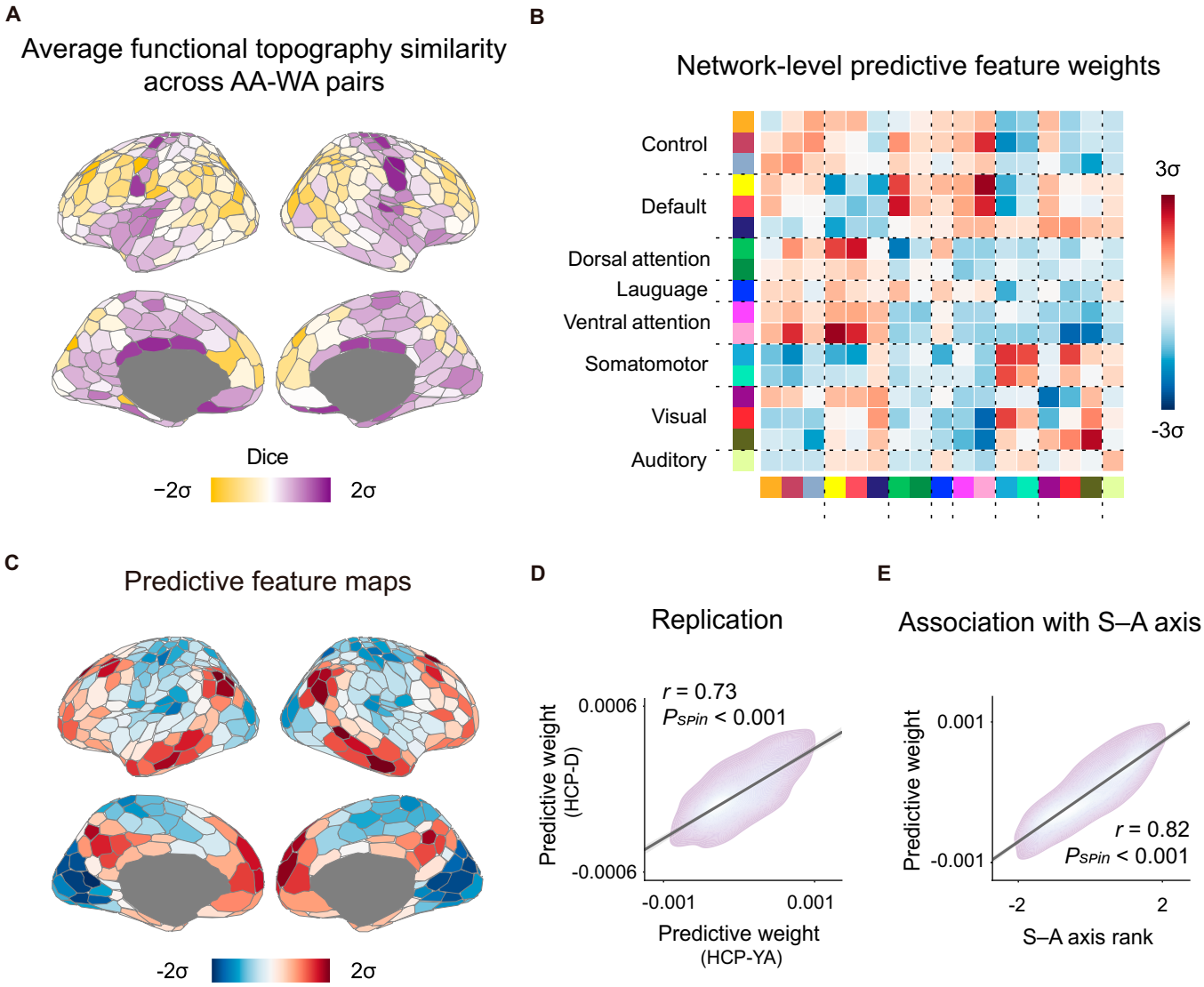


Fig. 1. Functional topography and functional connectivity are associated with ethnicity/race. (A) The average similarity of individual-specific parcellations across all the AA–WA pairs revealed that ethnicity/race-related topographic variability was greatest in heteromodal association cortices and lowest in the unimodal sensorimotor cortices. Brain maps were generated using the Schaefer400 parcellations [41] and visualized with the R package ggseg [115]. (B) Kernel ridge regression (KRR) models were trained using resting-state functional connectivity (RSFC) while controlling for age, sex, root-mean-square framewise displacement (RMS), intracranial volume (ICV), education, and income to predict individuals' self-reported ethnicity/race. Haufe-transformed regional pairwise feature weights were averaged to the network level based on the Yeo networks. Connections between default and attention networks, as well as within default networks and sensorimotor networks, contributed most to the prediction in both datasets. For visualization, actual values were subjected to *Z* score standardization. (C) Haufe-transformed weights of each brain region were averaged to generate ethnicity/race-predictive weight maps. (D) RSFC-based ethnicity/race prediction was performed in both the discovery HCP-YA dataset and the replication HCP-D dataset. Predictive weights were highly reproducible across the 2 independent datasets ($r = 0.73$, $P_{spin} < 0.001$, 2-sided). (E) Ethnicity/race-predictive weight distributions were significantly correlated with the S–A axis ranks ($r = 0.82$, $P_{spin} < 0.001$, 2-sided).

root-mean-square framewise displacement (RMS) [39]. To minimize sensitivity to particular data split, the above steps were repeated multiple times until 40 distinct AA splits with matched WA splits emerged. Multivariate kernel ridge regression (KRR) was employed to distinguish between AA and WA individuals, with RSFC matrices as predictors and age, sex, RMS, intracranial volume (ICV), education, and income as covariates [39,45]. Specifically, nested 5-fold cross validation was performed, with all the training folds used to optimize the regularization parameter and the remaining test fold to evaluate model generalizability on unseen data. Classification accuracy was averaged across folds for each split, and the entire 5-fold cross-validation procedure was repeated 40 times to ensure robust performance estimates (Fig. S3). In the HCP-YA dataset, our multivariate approach achieved high classification performance, with an accuracy of 85.3% ± 2.3% (mean ± SD) using individual-specific parcellations and 77.9% ± 2.6% using Schaefer400 parcellations, both significantly exceeding chance levels (both $P < 0.001$). In the HCP-D dataset, model performance decreased slightly but remained significantly above chance (both $P < 0.001$), with accuracies of 81.7% ± 5.0% for individual-specific parcellations and 62.5% ± 5.1% for Schaefer400 parcellations. These results emphasize the importance of treating individual-specific topographic features as phenotypes and highlight the robust ethnicity/race-related variability in functional topography and functional connectivity patterns.

To interpret the network features learned by the model, the regression models were inverted using Haufe's transform, yielding prediction feature matrices [46]. Figure 1B and Fig. S4 show the averaged pairwise region-level feature weights at the network level, indicating that ethnicity/race-associated functional connections constitute a distributed set of large-scale network circuits. The most prominent links were observed between the default and attentional networks, within the default networks, and within the sensorimotor networks for both datasets. Moreover, to quantify regional contributions, average feature weights of cortical regions were calculated (Fig. 1C and Fig. S4). We found that discriminating features derived from the HCP-YA and HCP-D datasets exhibited high generalizability and significant spatial correlations (Fig. 1D; $r = 0.73$, $P_{spin} < 0.001$). Across both datasets, contribution weights followed a hierarchical distribution across the cortex, with opposite contributions between heteromodal cortices and unimodal cortices. This hierarchical layout, reflecting diverse neurobiological properties, corresponds to the well-established cortical sensorimotor–association (S–A) axis [47]. Using spatial permutation testing, we confirmed that the contribution of cortical regions to ethnicity/race prediction was aligned with the S–A axis (Fig. 1E; $r = 0.82$, $P_{spin} < 0.001$). Importantly, control analyses using 2 alternative lower-resolution parcellations (individual-specific 100- and 200-region cortical parcellations) showed highly similar predictive patterns (Fig. S5).

Ethnicity/race-related variability in brain functional connectome is constrained by the fundamental properties of brain organization

The spatial and physical patterns of brain anatomy are known to constrain neural dynamics [13]. Thus, we next examined whether ethnicity/race-related variability in functional connectivity could be explained by the corresponding variability in cortical morphology. To this end, we constructed an MSN for each individual, which integrates multiple structural MRI features (Z scores) into a biologically meaningful and behaviorally relevant connectome [15,48]. Correlation weights were averaged across rows and within groups to generate group-level regional MSN values (Fig. 2A). To assess ethnicity/race-related variability in brain morphology, linear regression models (LRMs) were applied while controlling for age, sex, RMS, ICV, education level, income, age × sex, and education × income [39]. We observed significant ethnicity/race-related variations in morphometric similarity patterns across the cortex (Fig. 2B and Fig. S6; mean partial $R^2 = 0.03$), especially in the insula, prefrontal cortex, cuneus, and lateral occipital cortex. Importantly, this variability was highly reproducible across datasets (Fig. 2C; $r = 0.59$, $P_{spin} < 0.001$). Moreover, the MSN t-map was positively associated with the RSFC-based ethnicity/race predictive weights (Fig. 2D; $r = 0.41$, $P_{spin} = 0.012$), indicating that brain regions contributing more to RSFC-based predictions also exhibited greater ethnicity/race-related variability in cortical morphology.

Beyond the MSN, we considered other fundamental properties of brain organization. Intracortical myelination, a microstructural marker of neuronal fibers that influences processing efficiency in the nervous system [49,50], was estimated from the ratio of T1-weighted to T2-weighted images, where higher values reflect greater myelination. Across the cortex, predictive weight maps were inversely related to the cortical myelin content (Fig. S7; $r = -0.57$, $P_{spin} < 0.001$). Together, these results demonstrate that ethnicity/race-related variability in brain functional connectivity is tightly linked to fundamental structural properties of brain organization.

Lifestyle influences ethnicity/race-related variability in brain functional connectome

Lifestyle factors, including education, income, alcohol consumption, smoking, sleep, physical activity, and social connection, have been shown to influence brain structure and function [51–55]. Having revealed the ethnicity/race-related variability in RSFC architecture, we next sought to investigate the role of these lifestyle factors in explaining this variability [56]. Specifically, our goal was to identify the shared brain-network features that are associated with both ethnicity/race and various lifestyle factors. We selected 6 lifestyle factors (i.e., education, income, substance use, sleep, physical activity, and social relationships; Table S2) from the HCP-YA dataset, and we did not conduct the subsequent analysis for the HCP-D dataset as the majority of lifestyle data were only available for a subset of participants (e.g., those under age 17), which would substantially reduce the AA sample size. We found that several lifestyle factors were significantly associated with ethnicity/race categories in the HCP-YA dataset: education ($r = -0.15$, $P < 0.001$), income ($r = -0.23$, $P < 0.001$), substance use ($r = -0.08$, $P < 0.05$), sleep ($r = 0.11$, $P < 0.01$), physical activity ($r = -0.18$, $P < 0.001$), and social relationships ($r = -0.08$, $P < 0.05$).

Furthermore, all the HCP-YA participants were randomly split into 5 folds, with the constraint that participants from the same family were kept together in the same fold. To minimize sensitivity to any particular data split, this procedure was repeated 40 times. Using KRR models, we showed that all these factors could be predicted significantly above chance from RSFC matrices, with prediction accuracies of 0.18 ± 0.02 for education, 0.10 ± 0.02 for income, 0.19 ± 0.02 for substance use, 0.08 ± 0.03 for physical activity, 0.06 ± 0.02 for sleep, and 0.06 ± 0.02 for social relationships (Fig. 3A; Pearson's coefficient was employed as a prediction performance metric). Moreover, we examined the similarity of Haufe-transformed predictive network features underlying ethnicity/race and each lifestyle factor. Strong correlations were observed for education ($r = -0.61$, $P < 0.001$), income ($r = -0.70$, $P < 0.001$), substance use ($r = -0.26$, $P < 0.001$), physical activity ($r = -0.50$, $P < 0.001$), and sleep ($r = 0.48$, $P < 0.001$), but not for social relationships (Fig. 3B; $r = 0.06$). Predictive network feature matrices for all the lifestyle factors are shown in Fig. S8. Finally, by leveraging data capturing the impacts of neighborhood-level socioeconomic environments on intrinsic brain activity reported by Sydnor et al. [47], we demonstrated that the observed ethnicity/race-related variability aligns with brain–environment associations across the cortical mantle (Fig. 3C; $r = 0.57$, $P_{spin} < 0.001$ in the HCP-YA dataset; $r = 0.41$, $P_{spin} = 0.002$ in the HCP-D dataset), suggesting ethnicity/race-by-environment interaction effects that shape brain functional organization.

Next, we fitted a structural equation model (SEM) for each lifestyle factor to analyze the relationships among ethnicity/race group, lifestyle, and brain functional organization (represented by the principal functional gradient) while controlling for age, sex, RMS, and ICV (Fig. 3D). The principal functional gradient captures the dominant patterns of cortical variability in RSFC, explaining approximately 23.4% of the total variance (Fig. S9). Validation analyses confirmed that this gradient

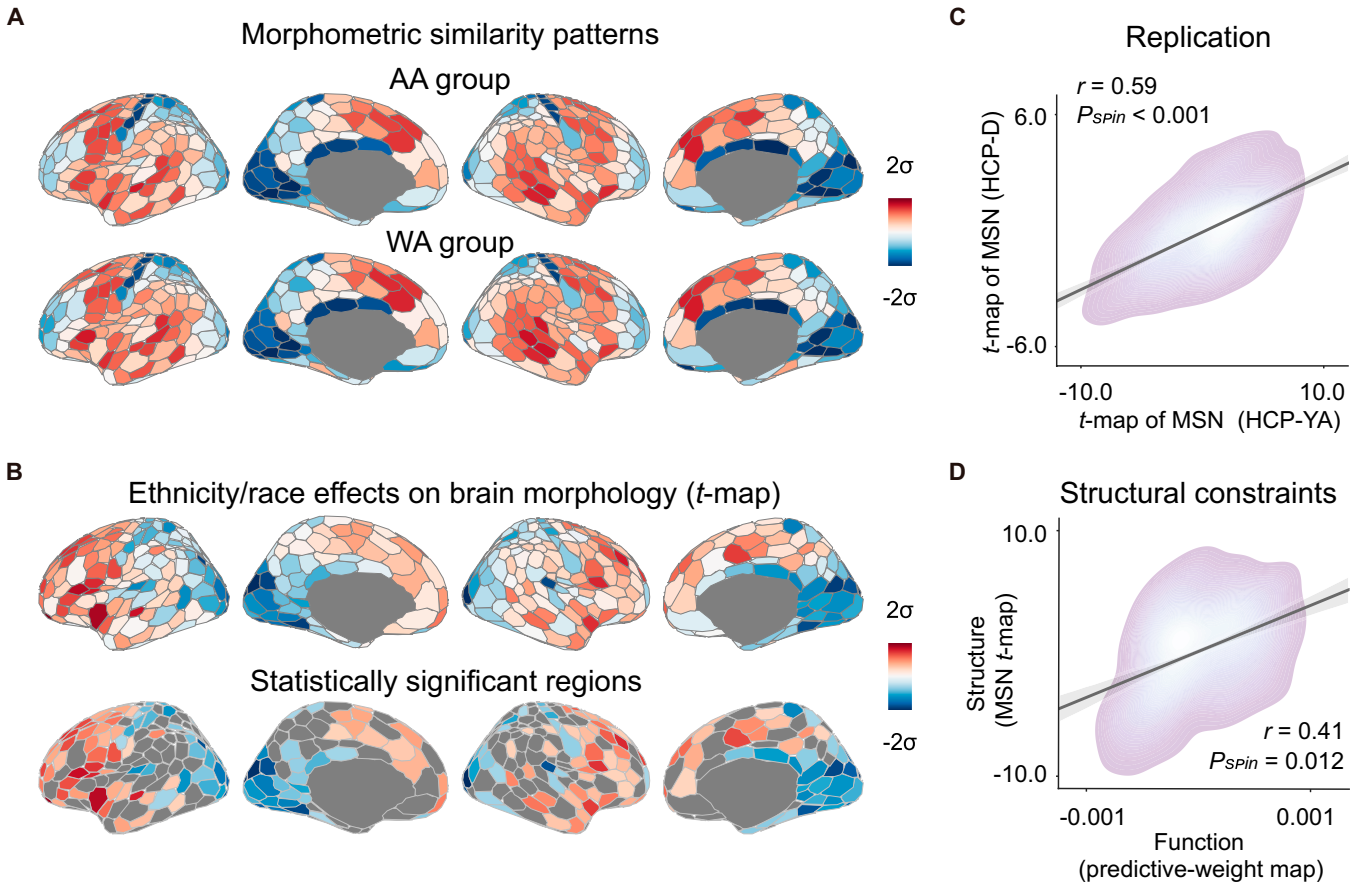


Fig. 2. Ethnicity/race-related variability in functional connectivity profiles aligns with ethnicity/race-related variations in cortical morphometry. (A) The cortical distribution of mean regional morphometric similarity network (MSN) values was examined, reflecting inter-regional similarity across multiple MRI-derived morphometric features (i.e., cortical thickness, gray matter volume, surface area, Gaussian curvature, and mean curvature). Brain maps were generated using the Schaefer400 parcellations [41] and visualized with the R package ggseg [115]. (B) Comparison (*t*-map) of regional MSNs across ethnic/racial groups was performed. Linear regression models (LRMs) were fitted to estimate the ethnicity/race-related variations in the MSN, controlling for age, sex, RMS, ICV, education, income, age × sex, and education × income. False discovery rate (FDR) correction with $P < 0.05$ for multiple comparisons across 400 regions identified significant ethnicity/race-related effects on cortical morphometry. (C) The *t*-map for regional MSN differences was highly reproducible across the 2 datasets ($r = 0.59$, $P_{spin} < 0.001$, 2-sided). (D) Ethnicity/race-related variability in cortical morphometric similarity accounted for parts of the variance in ethnicity/race-relevant variability in functional connectivity profiles ($r = 0.41$, $P_{spin} = 0.012$, 2-sided).

preserves substantial inter-individual information (Fig. S10; r = 0.65), retains the majority of ethnicity/race-related predictive information (Fig. S11), and offers a robust low-dimensional representation of brain functional organization (Fig. S12) [57]. The regression coefficients in the converged SEM suggested that ethnicity/race category was a significant predictor for education ($\beta = -0.353$, $P_{FDR} < 0.01$), substance use ($\beta = -0.365$, $P_{FDR} < 0.001$), and income ($\beta = -0.575$, $P_{FDR} < 0.001$). In turn, education ($\beta = 0.080$, $P_{FDR} = 0.020$), substance use ($\beta = 0.072$, $P_{FDR} < 0.001$), and income ($\beta = 0.080$, $P_{FDR} = 0.013$) were significant predictors for brain function, indexed by the first principal gradient of the RSFC profiles. Mediation analyses further revealed that education and substance use significantly mediated the associations between ethnicity/race category and brain function (Fig. 3B; 95% CI [−0.065, −0.005] and [−0.047, −0.014], respectively). No other mediation effects remained consistently significant across both the main and sensitivity analyses (Fig. S12).

Given the mediating roles of education and substance use, we further investigated how their interactions with ethnicity/race influence brain functional organization across the cortical mantle using LRMs (Fig. 3E). We found that the cortical regions significantly modulated by the ethnicity/race–education and ethnicity/race–income interactions exhibited substantial spatial overlap, primarily involving the insula and opercular cortex, inferior parietal lobule, inferior frontal cortex, dorsolateral prefrontal cortex, lateral temporal cortex, and anterior cingulate cortex. Additionally, cortical regions significantly influenced by ethnicity/race–substance use interactions were predominantly located in the posterior insula, posterior cingulate cortex, superior parietal lobule, and prefrontal cortex.

Cortical gene expression related to ethnicity/race-induced variability in brain functional connectome

After demonstrating the influence of lifestyle factors on ethnicity/race-related variability in RSFC profiles, we next aimed to identify the transcriptional signatures associated with this variability. Brain-wide gene expression data were obtained from the AHBA (http://human.brain-map.org) [58,59] and mapped into 400 region-level parcellations (400 regions × 9,110 genes) derived from the original 3,702 distinct microarray samples. Using partial least squares (PLS) regression [60], an advanced approach

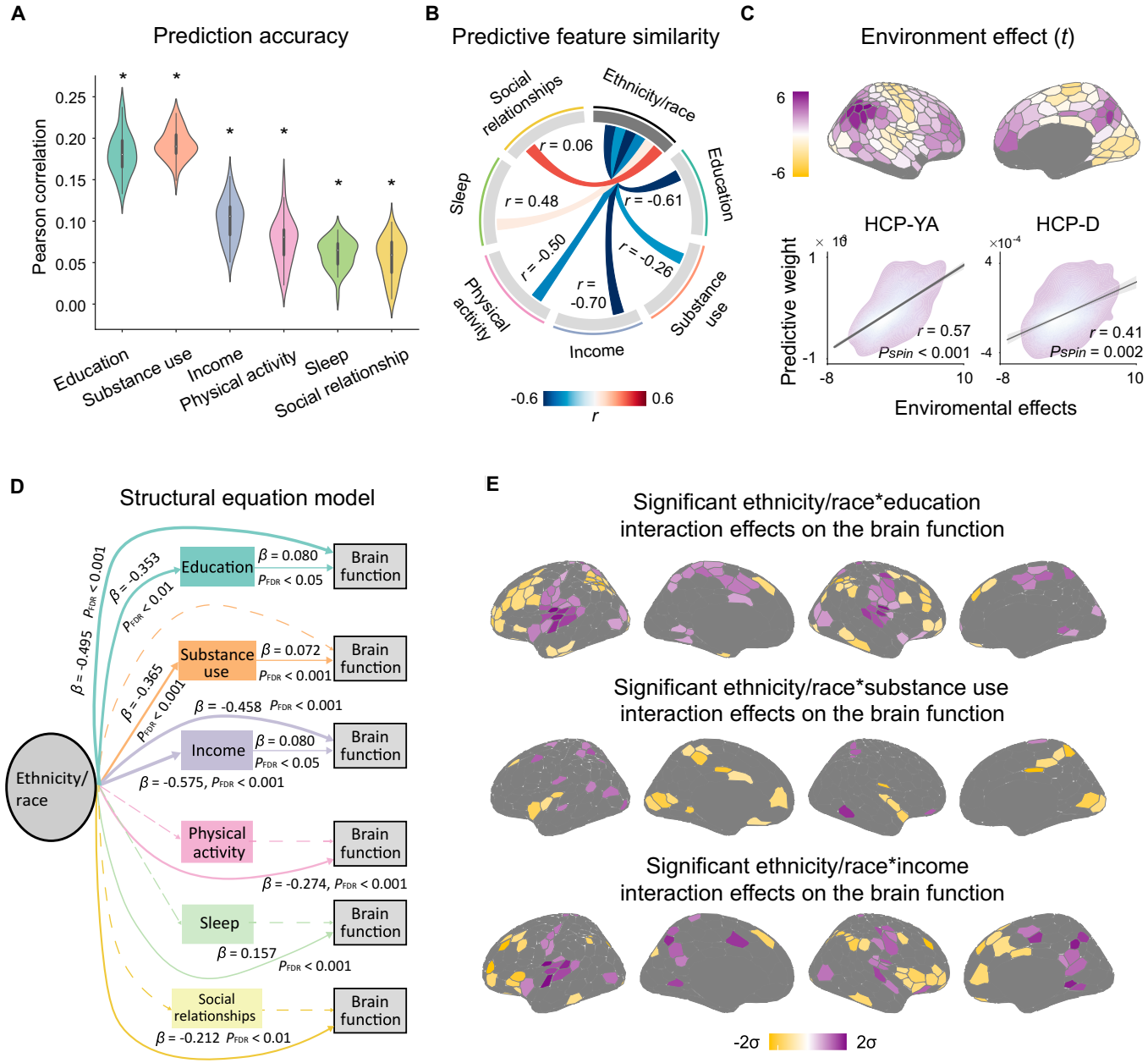


Fig. 3. Lifestyle factors mediate the associations between ethnicity/race and brain functional connectivity. (A) Mean prediction accuracies for lifestyle factors. Asterisks indicate above-chance predictions ($P_{perm} < 0.001$), determined by comparing true accuracy with 1,000 permuted null models. Violin plots display accuracy distributions across 40 replications. For each violin plot, width represents the density of the accuracy values, and the central box shows the interquartile range and median. (B) Correlations of predictive feature matrices between ethnicity/race and lifestyle factors, indicating shared brain-network features underlying both ethnicity/race and lifestyle predictions. (C) Functional connectivity-based ethnicity/race predictive features were significantly associated with effects of neighborhood socioeconomic conditions on the intrinsic brain activity (HCP-YA dataset: $r = 0.57$, $P_{spin} < 0.001$; HCP-D dataset: $r = 0.41$, $P_{spin} = 0.002$; 2-sided). (D) A structural equation model was fitted for each lifestyle factor, thereby revealing the relationships between ethnicity/race, lifestyle, and brain functional organization while controlling for age, sex, RMS, and ICV. Edges represent regression coefficients (β values), with thickness proportional to their absolute magnitude. Significant links ($P_{FDR} < 0.05$) are shown as solid lines; nonsignificant links as dashed lines. Mediation analysis revealed that education and substance use significantly mediated the relationship between ethnicity/race and brain functional organization (95% bootstrap CI did not include 0). (E) Threshold β-maps from LRMs, showing statistically significant ($P_{FDR} < 0.05$) ethnicity/race–education, ethnicity/race–substance use, and ethnicity/race–income interaction effects on the brain functional organization.

for uncovering fundamental relationships between 2 high-dimensional matrices, we identified weighted cortical gene expression patterns that aligned with the spatial distribution of ethnicity/race predictive features. The first component (PLS1), which explained the largest proportion of variance, accounted for 38.3% ($P_{perm} < 0.001$) of the response variance in the HCP-YA dataset and 20.5% ($P_{perm} < 0.001$) in the HCP-D dataset.

We found that the PLS1-weighted maps revealed an anterior-to-posterior hierarchy pattern along the cortex, which was remarkably consistent across the 2 datasets ($r = 0.99$, $P_{spin} < 0.001$). Importantly, these spatial patterns remained highly stable across different data processing choices, including alternative intensity-based filtering thresholds (0.3, 0.5, and 0.7; Fig. S13) and multiple differential-stability (DS) thresholds (0, 0.1, and

0.2; Fig. S14). Moreover, PLS1 gene expression weights were strongly correlated with the ethnicity/race predictive weights (Fig. 4A; $r = 0.62$, $P_{spin} < 0.001$), suggesting that genes with higher positive (or negative) weights on PLS1 tend to be overexpressed in regions showing corresponding positive (or negative) ethnicity/race predictive weights. We then ranked the genes based on normalized PLS1 weights and selected those with $Z > 5$ (denoted as the PLS1$^+$ gene sets) and those with $Z < -5$

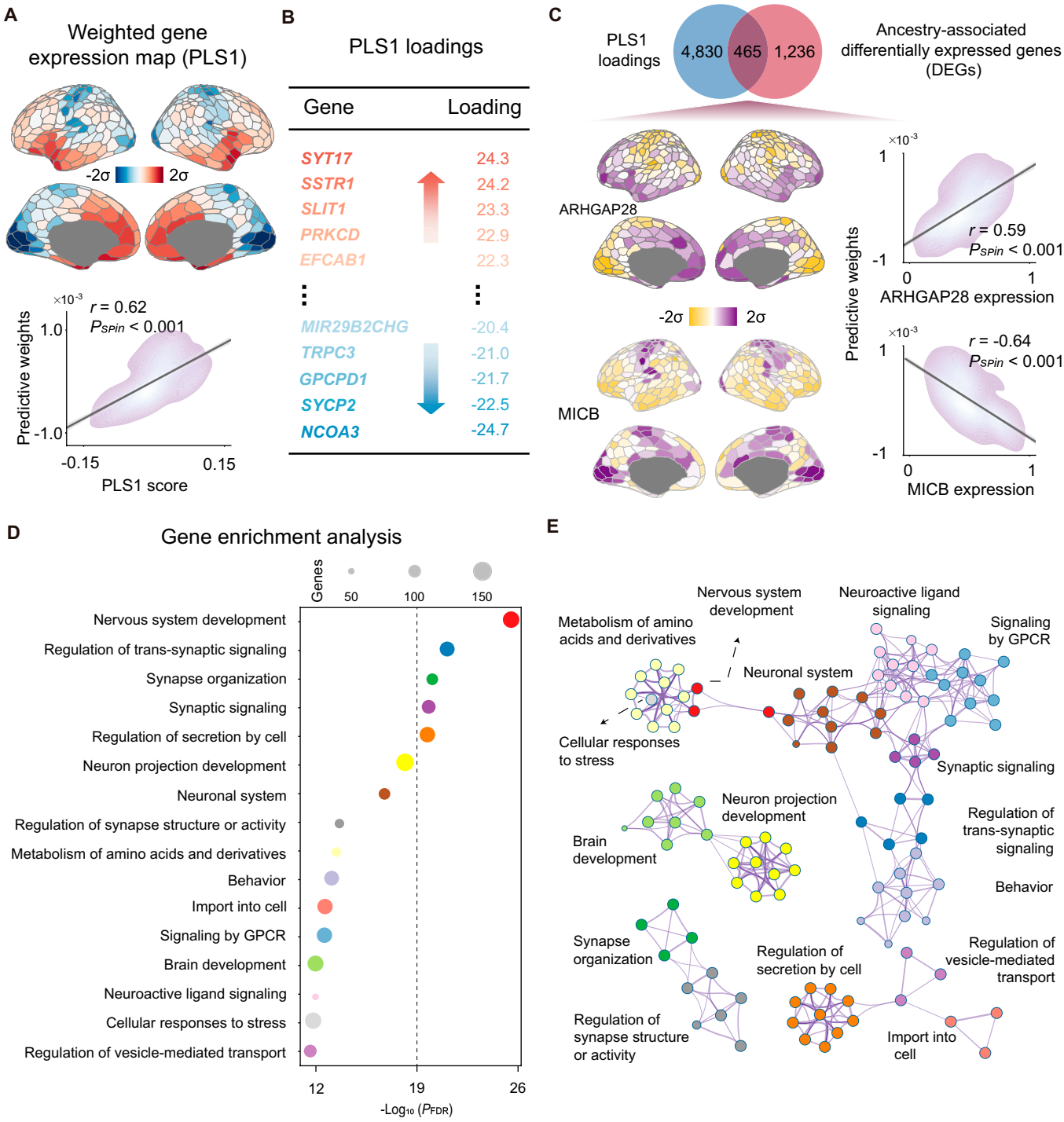


Fig. 4. Gene expression profiles associated with ethnicity/race-related variability in functional connectivity. (A) Weighted cortical gene expression map of the regional PLS1 scores (top panel). Scatterplot showing the relationship between the PLS1 map and the Haufe-transformed predictive weight map (bottom panel, $r = 0.62$, $P_{spin} < 0.001$, 2-sided). Brain maps were generated using the Schaefer400 parcellations [41] and visualized with the R package ggseg [115]. (B) Genes were ranked on the basis of their loadings on PLS1, and the complete PLS1 gene list is available in Data S1. (C) The PLS1 genes overlapped with ancestry-associated differentially expressed genes (DEGs) reported by Benjamin et al. [34]. (D) Representative enriched terms of the PLS1$^+$ genes, highlighting GO biological processes related to synaptic signaling, as well as Reactome gene sets associated with the nervous system. Circle size denotes the number of genes within a given ontology term, and multi-test FDR-adjusted P values are plotted as $\log_{10}$-transformed values. (E) Metascape network plot of enriched terms, capturing intra-cluster and inter-cluster similarity relationships. Each term is represented by a circle, colored by cluster identity and scaled proportional to the number of genes involved.

(denoted as the PLS$^-$ gene sets) for subsequent analyses (Fig. 4B and Fig. S15).

We next conducted an external validation by comparing our PLS1 gene set with the genetic ancestry-associated DEGs identified from RNA sequencing data of postmortem brain tissue [34]. Among the 1,701 DEGs, only 465 (~27.3%) overlapped with the PLS1 genes in the HCP-YA dataset (Fig. 4C). Given that ancestry-related gene expression is primarily driven by genetic variations (explaining ~60% of the changes) rather than the environments (~15%) [34], this limited overlap between the MRI-derived PLS1 genes and ancestry DEGs suggests that the transcriptional changes associated with self-reported ethnicity/race are largely distinct from those driven by genetic ancestry. One plausible explanation for this distinction is that the MRI-derived PLS1 gene signature is more strongly associated with environmental and lifestyle factors. Delving into the overlapping genes, ARHGAP28, which encodes the Rho guanosine triphosphatase (GTPase)-activating protein [61,62], exhibited the strongest positive correlation with ethnicity/race predictive weights (Fig. 4C; $r = 0.59$, $P_{spin} < 0.001$). In contrast, MICB, which encodes ligands for the natural killer cell-activating receptor NKG2D [63], exhibited the strongest negative correlation (Fig. 4C; $r = -0.64$, $P_{spin} < 0.001$).

To further interpret the PLS1$^-$ and PLS1$^+$ gene sets, we conducted gene enrichment analysis to characterize the enriched biological functions and pathways using Metascape [64]. After employing Benjamini–Hochberg correction for multiple hypothesis testing and discarding discrete enriched clusters, the remaining significantly enriched terms of the PLS1$^+$ genes were rendered into a network (Fig. 4D and E and Fig. S15), including gene ontology (GO) biological processes, such as "Regulation of trans-synaptic signaling" and "Synapse organization", as well as Reactome gene sets, such as "Neuronal system", "Nervous system development", "Metabolism of amino acids and derivatives", and "Signaling by GPCR". The PLS1$^-$ genes were enriched for GO biological processes, such as "Metal ion transport" and "mRNA metabolic process", as well as Reactome pathways, including "Neuronal system" and "Transport of small molecules" (Tables S3 to S10). Collectively, these results highlight the distinct functional roles of genes with positive versus negative weights on PLS1.

Discussion

In this study, we presented a multi-layered framework for understanding ethnicity/race-related variability in brain functional organization. Using multimodal datasets and precision individualized parcellation, we showed that hierarchical connectivity patterns from sensorimotor to association cortices predict ethnicity/race and align with structural variations across populations. Furthermore, we observed that the shared brain-network features served as predictors for both ethnicity/race and various lifestyle factors, with education and substance use substantially mediating the associations between ethnicity/race and brain connectivity. We also characterized the transcriptomic architectures underlying the observed ethnicity/race-related variability, thereby bridging the gap between macroscale functional connectomic diversity and microscale molecular signatures. Notably, the reproducibility across 2 large cohorts underscores the robustness of our findings and echoes recent calls for reproducible neuroscience research. Overall, our study integrates structural, behavioral, and molecular dimensions to provide a comprehensive biological perspective on population diversity and contributes to a more generalizable and equitable neuroscience.

Both the spatial configuration of functional regions and the coupling strength between regions are important drivers of variability in functional organization, which is closely linked to non-imaging measures of behavioral and lifestyle measures [65]. Here, we observed that both functional topography and connectivity are associated with individuals' ethnicity/race. First, spatial variation in functional topography across ethnicity/race groups was greater in heteromodal association cortices than in unimodal sensorimotor cortices. This finding extends previous findings showing that association networks exhibit the greatest variations in functional topography across age windows [66], sex [67], and cultural populations [12]. Second, multivariate patterns of brain–ethnicity/race associations were inversely driven by the connectivity profiles of higher-order association regions versus modality-specific regions, indicating that ethnicity/race-related sociodemographic factors exert widespread and opposite effects on the 2 poles of the S–A axis [47]. Additionally, ethnicity/race-related differences in functional connectivity profiles were closely aligned with variations in morphometric similarity across groups. This suggests that functional connectivity differences associated with ethnicity/race are constrained by brain morphology, conforming with the well-established concept of cortical structural constraints on intrinsic neuronal activity [13,68]. These findings further support the homophilic principle of brain organization, which posits that brain regions with similar functional characteristics are more likely to share similarities across multiple biological domains and to be connected via white matter tracts [69].

Given the multidimensional properties of ethnicity/race, a comprehensive perspective is needed to link ethnic/racial diversity with the hierarchical functional organization of the brain [39]. Recent compelling evidence demonstrates that children's neighborhood environments exert opposing effects on the fluctuation amplitude of intrinsic activity within the sensorimotor and association cortices [47]. Socioeconomically disadvantageous environments diminish the differentiation of the S–A hierarchy [47]. In this study, we demonstrated that these environmental effects are spatially aligned with ethnicity/race-related variability, suggesting an overlap between ethnicity/race and various socio-environmental factors. Moreover, it is well-established that environmental and lifestyle factors can shape both brain structure and function [53,54,70]. Building on this, our findings reveal that shared functional network features underlie both lifestyle factors and ethnicity/race. Specifically, connections between the control and somatomotor networks, between the default and ventral attention networks, and within the somatomotor network were strongly associated with both education level and ethnicity/race. In addition, connections within the default networks, between the default and dorsal attention networks, and between the default and ventral attention networks were robustly predictive for both the substance use experience and ethnicity/race. Indeed, behavior prediction models may capture broad behavior dimensions within a given behavioral domain rather than the specific traits they are trained on, such as the *g* factor in the case of cognition and the *p* factor in the case of mental health [45]. Thus, the observed similarity of predictive network features suggests that the ethnicity/race variable and lifestyle factors may be supported by shared underlying meta-factors [71].

Moreover, we found that lifestyle factors—particularly education and substance use—significantly mediated the associations

between functional connectivity profiles and ethnicity/race. This is particularly relevant as prior studies have shown that educational attainment and rates of substance use (especially marijuana and alcohol) differ across ethnic/racial populations [17,72–74]. The principal functional gradient of regions located in the insula and prefrontal cortex was significantly influenced by the interactions between ethnicity/race and education, as well as by the interactions between ethnicity/race and substance use. These regions serve as crucial control hubs of top-down information processing [75] and overlap with circuits implicated in emotional regulation and threat responses [76,77]. Moreover, both education and substance use are important components in pathways linking the environment and health status [54,78]. Educational background is often linked to cognitive reserves [79]. Higher levels of education may enhance brain's flexibility and adaptability during task processing and decision-making [80,81], and protect neurogenerative risks [82,83] in later life. Excessive substance use alters the neurobiology of reward processing, control dynamics, and emotion regulation [84–86] and is associated with psychiatric conditions, particularly depression symptoms, and reduced quality of life [87–90]. Together, our findings provide insights into how ethnicity/race-related social constructs are biologically embedded in the brain and suggest that fully accounting for socioenvironmental disadvantages of specific populations is essential for interpreting neuroimaging-derived differences across populations and for developing more generalizable interventions. Although the lifestyle factors analyzed here were relatively coarse, they significantly mediated the observed ethnicity/race-related variability, underscoring the need for future work to incorporate more comprehensive measures of lifestyle (e.g., access to healthcare) and neighborhood-level environment (e.g., population density or percentage of residents living in poverty) to more fully elucidate ethnicity/race-related variability in brain organization and brain–behavior relationships and to promote equitable translation of neuroscience findings. Finally, although we modeled lifestyle and transcriptomics, "nature and nurture can hardly be disentangled" completely in our cross-sectional study. Therefore, the identified associations should be interpreted not as inherent biological divergences but as the neurobiological embedding of specific sociocultural experiences.

After linking functional network properties to transcriptomic data, we identified a set of genes (PLS1) whose weighted cortical expression patterns were significantly correlated with ethnicity/race-related variability in functional connectivity. The PLS1 gene expression map revealed high expression in the primary visual, anterior cingulate, and insular cortex, following the global cortical hierarchy of the brain. Gene-to-function annotation analysis revealed that these genes formed a topologically clustered network enriched for several GO biological processes and Reactome pathways in both the HCP-YA and HCP-D cohorts. The identified GO terms were primarily related to synaptic organization and the regulation of trans-synaptic signaling, which underpin inter-neuronal communication and information processing in the nervous system [91]. Mechanistically, variations in these synaptic-related processes may modulate the efficacy of neurotransmission and the excitation–inhibition balance within local circuits, which are fundamental for maintaining the integrity of large-scale functional circuits [92,93]. Moreover, this enrichment is consistent with prior reports of population differences in gene expression associated with axon guidance and synaptic signaling pathways [35]. The identified Reactome pathways included the neuronal system and its development, which encompass neuronal progenitor cell proliferation, migration, differentiation, synaptogenesis, and synaptic pruning—all fundamental for establishing a mature and integrated neural system [94–96]. Importantly, many of these neurodevelopment-related pathways are influenced by environmental and lifestyle factors, such as socioeconomic status [97], alcohol consumption [98], early-life stress [99], and physical activity [100,101]. Thus, these identified molecular architectures may serve as the biological interface where cumulative environmental experiences associated with ethnicity/race (e.g., chronic stress) are integrated into the brain's functional architecture. Collectively, these findings bridge the critical gap between ethnicity/race-related variability in brain functional organization and the underlying transcriptional programs. By delineating these molecular mechanisms, we demonstrate that population-related differences in functional organization are supported by specific neurodevelopmental and synaptic molecular signatures. This highlights brain functional topography and connectivity as important intermediate phenotypes that link molecular variation to macroscale diversity, offering a mechanistic framework for understanding the neurobiological context of behavioral variability and potential health disparities.

Several limitations of the current study should be considered when interpreting our findings. First, the generalizability of our findings is constrained by the nature of the datasets used. Our population sample was limited to self-identified WA and AA participants from the United States. Ethnicity/race is a social construct deeply embedded in specific cultural and historical contexts, reflecting systemic disparities in public sector investment, healthcare access, and socioeconomic status that are unique to specific nations [16,102]. This makes it challenging to generalize our conclusions across the full spectrum of ethnicity/race populations. Future work needs to validate these mechanisms in global diverse populations to avoid essentializing group differences and to better understand the complex interplay between structural inequality and brain organization [102]. Second, by using 2 independent cross-sectional cohorts (HCP-YA and HCP-D) that differ in scanner protocols, we were unable to explicitly model developmental trajectories of ethnicity/race-related differences. Longitudinal datasets, such as the Adolescent Brain Cognitive Development (ABCD) study, are needed to investigate how these brain-wide associations evolve across developmental stages. Third, the transcriptome–neuroimaging associations are limited by the small, demographically skewed sample (a sample of 6 donors—1 Hispanic, 2 AA, 3 Caucasian—only 2 of whom provided data for the right hemisphere) of the AHBA gene expression dataset. Future work should move toward integrating individual-level genetic data with more comprehensive, longitudinal characterizations of lifestyle and environmental exposures. Finally, regarding methodology, while our correlation-based brain morphology network and KRR approaches are robust and widely validated, future studies could benefit from employing more advanced divergence-based approaches, such as Morphometric INverse Divergence (MIND), to delineate individualized connectomes of brain morphology [103,104], and using nonlinear representation learning models to characterize complex brain–behavior relationships [105,106]. These methods may provide complementary and deeper insights into the population-level and inter-individual variability in the human brain, further advancing the field.

Despite these limitations, our study provides a multi-layered perspective for understanding ethnicity/race-related influences

on brain functional organization by weaving evidence from structural constraints, lifestyle factors, and transcriptomic signatures. By integrating these dimensions, we move beyond simplistic explanations of population-level brain differences and highlight the multidimensional nature of ethnicity/race. Ultimately, our findings advocate for a fundamental shift in perspective: from treating ethnicity/race as a simple causal variable to conceptualizing it as a complex construct whose effects on the brain are deeply entangled with a confluence of biological and environmental influences.

Methods

Datasets

This study utilized 2 publicly available datasets from the HCP: the HCP-YA and HCP-D datasets. The HCP-YA participants (N = 822; age: 22 to 37 years) were part of the HCP S1200 release [107] and matched the HCP subset used by Li et al. [39]. Rs-fMRI data were acquired during 2 sessions using a multiband sequence (voxel dimension: 2.0 mm isotropic; repetition time: 0.72 s) on a customized Siemens 3-T Skyra at Washington University in St. Louis. Each session comprised 2 runs with opposite phase-encoding directions, and the duration of each run was approximately 14.4 min. Structural images were acquired for each participant with a resolution of 0.7 mm isotropic. Family structures and self-reported ethnicity/race information were carefully considered in subsequent processing. HCP-D participants (N = 472; age: 5 to 21 years) were obtained from the lifespan HCP release 2.0 [108]. For participants 8 years and older, rs-fMRI data were acquired during 2 sessions using a multiband sequence (voxel dimension: 2.0 mm isotropic; repetition time: 0.80 s) on a 3-T Siemens Prisma scanner. Each session encompassed 2 runs with opposite phase-encoding directions, and the duration of each run was approximately 6.5 min. For the youngest participants (5 to 7 years), the total duration of rs-fMRI scanning was reduced to 21 min. Informed consent was obtained from all participants aged 18 and older; for participants younger than 18, informed permission was provided by their parents. Both the HCP-YA and HCP-D datasets were approved by the Institutional Review Board (IRB) at Washington University in St. Louis. Additional details of the data collection process and behavioral measures can be found elsewhere. All procedures in this study were conducted following the applicable guidelines and regulations, with approval from the IRB at the Beijing Institute of Technology.

Image acquisition and processing

ICA-FIX denoised rs-fMRI data, which had undergone the minimal preprocessing steps of the HCP, were employed [109]. To improve the behavioral prediction performance, additional motion censoring and global signal regression were performed following the procedure described by Li et al. [39]. Specifically, volumes with an RMS exceeding 0.2 mm were marked as censored frames. Frames immediately preceding and the 2 frames following these volumes, as well as any previously uncensored segments shorter than 5 volumes, were also marked as censored frames. Rs-fMRI runs were discarded if more than half of the frames were marked as censored. Next, the signal of the remaining uncensored frames was averaged across the cortical vertices to generate the global signal. The global signal and its first temporal derivative were regressed out from the original time courses.

Defining individual-specific cortical parcellations and the functional connectome

The gMS-HBM approach was employed to define individual-specific cortical parcellations for each participant (https://github.com/ThomasYeoLab/CBIG/tree/master/stable_projects/brain_parcellation/Kong2022_ArealMSHBM) [40]. The steps of the gMS-HBM approach are as follows: (a) The Connectome Workbench (https://github.com/Washington-University/workbench) is used to compute each individual's diffusion embedding matrices for gradients; (b) connectivity profiles for each seed region, initialization parameters, and a probability spatial mask are generated; (c) group-level priors are estimated for each ethnicity/race group on the basis of the Schaefer400 parcellations [41] and 40 independent participants; and (d) Bayesian model estimation is performed for the generation of individual-level parcellations. The mathematical details of the gMS-HBM approach are described elsewhere [40]. Both individualized and Schaefer400 parcellations were then used to compute the RSFC matrices. The vertex-wise time series, excluding the censored frames, were averaged across all the regions of interest (ROIs). For each run, the RSFC matrix was obtained across 400 regions using Pearson's correlation analysis. The RSFC matrices were then Fisher z-transformed and averaged across runs, yielding 2 final 400 × 400 RSFC matrices for each participant.

Predictive modeling

Predictive modeling was based on the 5-fold cross-validation scheme. For the ethnicity/race prediction, AA participants within each of the HCP-YA and HCP-D datasets were randomly split into 5 folds, and participants from the same family were kept together in the same fold. Hungarian matching was then applied to select demographically matched AA–WA pairs based on age, sex, and RMS within each fold [39]. For the lifestyle factor prediction, all HCP-YA participants were randomly split into 5 folds, where the family structure was taken care of. To ensure the generalizability of our findings, the entire data splitting and matching process for both tasks was repeated 40 times.

Following these data preparation steps, we applied nested 5-fold cross-validated KRR models to predict ethnicity/race and various lifestyle factors separately. Our nested cross-validation consisted of an outer 5-fold loop for evaluating generalizability and an inner 5-fold loop, performed only within the outer-loop training folds, for tuning the regularization parameter. For each lifestyle factor, a composite score was generated before model training. This was achieved by averaging all related measures (Table S2) for each individual. KRR models perform the prediction for test participants by leveraging the similarity of their RSFC patterns to those of the training participants. Specifically, the prediction for a given test participant was calculated as the weighted average of the behavioral scores from all training participants, where the weights were determined by the Pearson's correlation between the vectorized RSFC matrices of the test participants and each training participant.

For each outer test fold, all steps involving parameter estimation, including covariate regression and kernel construction, were performed exclusively within the 4 training folds. All parameters determined within the training folds were subsequently used to make predictions for participants in the held-out test set. Within each outer-loop training set, an inner 5-fold cross-validation was performed to identify the optimal $l2$ regularization parameter (λ) for the KRR model to reduce overfitting.

The training set of the outer loop was further split into 5 inner folds. For each candidate λ, the model was trained on 4 inner folds and validated on the remaining one. This process was repeated across all inner folds, and the λ that yielded the best average inner-loop prediction performance was selected.

To mitigate potential sensitivity to data splitting variations, the entire nested cross-validation process was repeated 40 times. Additionally, when variables other than education and income were predicted, age, sex, RMS, ICV, education, and income were included as covariates and regressed out from the features. In contrast, when predicting education and income, age, sex, RMS, and ICV were included as covariates and regressed out from the RSFC features.

For the ethnicity/race prediction models, accuracy of each test set was defined as the proportion of correctly predicted samples to the total number of samples. For the lifestyle factor prediction models, the accuracy of each test set was determined using Pearson's correlation between the predicted and actual scores. The accuracy measures were averaged across all the folds for each data split, yielding 40 final prediction accuracy values. To rigorously assess whether the prediction performance was statistically significant, a corresponding set of null models was generated for each predictive model. Specifically, the output variable was permuted 1,000 times. This shuffling procedure effectively breaks the intrinsic link between brain and behavior, thereby generating an empirical null distribution under the null hypothesis of no association. For each permutation, a null model was trained and tested following the same procedures applied to the original model. The significance (*P* value) of each model was defined as the proportion of null models whose prediction accuracies exceed those of the true models.

Predictive feature weights

The Haufe transformation was used to interpret the brain–behavior relationships learned by the prediction models [46]. Because the regression weights obtained from KRR reflect the decoding solution optimized for prediction rather than the true contribution of each feature, they cannot be directly interpreted. To illustrate the necessity of the Haufe transformation, consider a hypothetical scenario where 2 functional connections, *FC1* and *FC2*, jointly produce perfect predictions [45]. Assume $FC1 = Y -$ noise and $FC2 =$ noise, and the optimal prediction model would be $\hat{Y} = 1 \times FC1 + 1 \times FC2$, assigning identical weights to both connections. Directly interpreting these weights would incorrectly suggest that both connections are equally related to the behavior. Haufe's inversion resolves this interpretability issue by transforming decoding weights into activation patterns computed via the covariance between each input feature and the predicted output. In the example above, the covariance between *FC2* and the predicted output would approach zero, correctly reflecting that *FC2* is unrelated to the target behavior.

Specifically, for each training fold, Haufe-transformed feature weights were calculated as the covariance between the demeaned RSFC features ($RSFC_{train}$) and the output predicted scores (y'_{train}). The feature weight matrices were averaged across the 40 splits to obtain the final importance measures (400 × 400), reflecting the contribution of each edge to the prediction. We subsequently summarized the pairwise Haufe-transformed weights to the network level (17 × 17). In addition, regional importance was calculated by averaging these weights for each of the 400 regions (400 × 1). In this study, we preserved the original positive and negative signs of the feature weights rather than taking their absolute values [110].

Morphometric similarity analysis

The Scharfer400 parcellation was transformed into the T1w surface space of each participant, and 5 morphometric features were extracted from the participant's T1w images for each region, including cortical thickness, gray matter volume, surface area, Gaussian curvature, and mean curvature [33]. For each participant, each morphometric feature was subjected to *Z*-normalization across regions, and a feature vector (5 × 1) was created for each region. Pearson's correlation analysis was then employed to estimate the morphometric similarity between cortical regions, yielding a pairwise MSN (400 × 400) for each participant. The full MSN matrices were then averaged across rows to generate a regional MSN map.

To visualize the spatial pattern of the MSN across the cortex, the regional MSN maps were averaged across participants within each ethnicity/race group. To examine the ethnicity/race-related variations in the MSN, an LRM was fitted for each region. These models used the regional MSN value as the response variable and included age, sex, RMS, ICV, education, income, age × sex, and education × income as covariates. Weights were applied to account for differences in group sizes, with each participant assigned a weight equal to the reciprocal of the size of their corresponding group. Two-sided *t* statistics were extracted from the LRMs, and significance was determined at $P < 0.05$ with the application of Benjamini–Hochberg false discovery rate (FDR) correction for multiple comparisons across the 400 regions to control for type I errors.

Structural equation modeling

The lavaan package (version 0.6.18) in R was used to fit a SEM for each lifestyle factor and estimate the regression coefficients for each path while controlling for age, sex, RMS, and ICV [53,54]. The complete model equations are provided in the Supplementary Materials. The composite score for brain function was derived from the participants' principal functional gradient. In this study, we applied principal components analysis (PCA) to the RSFC matrix of each participant for dimensionality reduction, and the resulting first principal component was identified as the principal functional gradient. The measure for brain function was subsequently constructed by averaging the *Z*-normalized gradient values of the top 15 cortical regions that were most significantly correlated with each lifestyle factor [53]. Before being entered into the model, we subjected the RMS, ICV, and lifestyle factors to *Z*-normalization to avoid scale effects and facilitate coefficient comparisons across models. The *P* value for each path was calculated by dividing the estimated parameter by its bootstrap standard error (SE). The *P* values of all paths within each SEM were then subjected to Benjamini–Hochberg FDR correction to account for multiple comparisons. Significance of the mediation effects ($a \times b$) was assessed using 95% bias-corrected bootstrap confidence intervals (CIs) based on 1,000 resamples; effects were considered significant if the CI did not include zero.

Interaction effects modeling

To examine how the ethnicity/race-related variability in brain functional connectivity is moderated by the socioeconomic status and substance use status of participants, we fitted 3 LRMs

for each region. These models controlled for age, sex, RMS, ICV, and age × sex and included an interaction term between ethnicity/race and either education, income, or substance use [111]. The response terms of these models were the regional principal functional gradient value, defined as the principal components derived from the RSFC matrix dimensionality reduction using PCA. Moreover, 2-sided t statistics for the interaction terms were extracted from the LRMs, and significance was determined at $P < 0.05$, with the application of Benjamini–Hochberg FDR correction for multiple comparisons across 400 regions to prevent type I errors. The complete model equations are provided in the Supplementary Materials.

Transcriptomic analysis

We utilized gene expression data from the AHBA dataset, derived from 6 postmortem brains (age: 24 to 57 years; 1 female) and comprising 3,702 spatially distinct samples. The preprocessing steps were performed according to the approach of Markello et al. [112]. These steps are as follows: (a) Probe-to-gene annotations were first updated, followed by intensity-based filtering with a threshold of 0.5 to select probes with the most consistent patterns of regional variation across donors, after which probes were aggregated to genes; (b) gene expression samples were mapped to the Schaefer400 parcellation, in which a bidirectional mirroring approach across the left and right hemispheres was applied, and centroid-based imputation was employed to address missing data; (c) the expression values of each sample were normalized across the genes for each donor, and subsequently, the expression values of each gene were normalized across all samples for each donor; and (d) the samples were aggregated across donors to generate expression values for a given region. We finally quantified the DS of each gene, defined as the consistency of its gene expression pattern across donor brains, measured using the Spearman's rank correlation. We retained genes with DS > 0.1, resulting in 9,110 genes for downstream analyses.

PLS regression was employed to relate the Haufe-transformed ethnicity/race predictive weights to the transcriptomic measurements of all 9,110 genes [33]. In the PLS model, Z-normalized gene expression data served as the predictor variable, and Z-normalized predictive weights served as the response variables. PLS1 provides the optimal low-dimensional representation of gene expression profiles that co-vary most strongly with ethnicity/race-related variability in brain functional connectivity. The statistical significance of the variance explained by PLS1 was assessed by spatially permuting the response variables 1,000 times. Finally, bootstrapping was used to quantify the estimation errors for the PLS1 weight of each gene. A Z score for each gene was then calculated by dividing its weight by its bootstrap SE, enabling the ranking of genes based on their PLS1 contributions.

In both the HCP-YA and HCP-D datasets, genes with $Z > 5$ and $Z < -5$ were identified as the $PLS1^+$ and $PLS1^-$ gene sets, respectively [33]. Each gene set was then submitted separately to the Metascape website, an automated functional pathway enrichment tool that provides biological insights for the given gene list, using all *Homo sapiens* genes as the background gene set [64]. To validate the enrichment results, the PLS genes from the HCP-YA and HCP-D datasets were then entered into Metascape together to conduct a multi-gene list meta-analysis. This approach facilitates the understanding of pathways that are shared across gene lists or are unique to a specific gene list. All identified pathways were considered significant at $P < 0.05$, corrected for multiple comparisons by the Benjamini–Hochberg FDR. To ensure that the enrichment results were not driven by spatial dependencies in brain gene expression, we further assessed the robustness of all reported pathways using a spin-based ensemble null model [113]. Specifically, we generated surrogate maps that preserve the spatial autocorrelation structure of the predictive weight map, and computed an empirical null distribution of enrichment scores across these 1,000 spatial permutations.

Control analyses

We performed several additional control analyses to ensure robustness of our results. First, we generated individual-specific 100- and 200-region cortical parcellations using gMS-HBM, Schaefer100, and Schaefer200, and computed the corresponding 100 × 100 and 200 × 200 RSFC matrices for each participant. The ethnicity/race prediction analyses were then repeated using these alternative RSFC representations. Second, to account for variability in gene expression patterns across the 6 AHBA donors, we recomputed the weighted PLS1 gene expression maps using multiple DS thresholds (DS > 0 and DS > 0.2). In addition, we evaluated our results using alternative intensity-based filtering thresholds (0.3 and 0.7) to verify that our findings were not driven by the specific background noise cutoff. Third, we evaluated the robustness of the dimensionality reduction strategy. We extracted the first components using 2 nonlinear embedding methods (i.e., diffusion embedding and Laplacian eigenmaps) and compared them with PCA-derived first component to assess the consistency of the low-dimensional representations. We also performed representational similarity analysis (RSA) to assess the preservation of inter-individual variability and re-ran the ethnicity/race prediction using only the first principal component derived from PCA to evaluate the extent to which ethnicity/race-related variation is preserved in the low-dimensional RSFC representation. Additionally, we re-ran the entire dimensionality reduction and SEM procedure using thresholded RSFC matrices (retaining only the top 10% of connections) [114].

Statistical analyses

The spatial association between different cortical maps was assessed across parcels using 2-sided Pearson's correlation analysis. To account for distance-dependent spatial autocorrelation, which can lead to an overestimation of statistical significance, we implemented a spin test. Specifically, a null distribution was generated for each cortical feature by performing 1,000 random rotations of the corresponding feature map. Permutation P values were calculated as the proportion of times that the absolute value of the null correlation exceeded the absolute value of the observed correlation. Spin tests were implemented using the Neuromaps toolbox (https://github.com/netneurolab/neuromaps).

Acknowledgments

We thank the HCP team and Z. Cui for their support and help.
Funding: This work was supported by the National Natural Science Foundation of China (grant numbers 62336002, 62406025, and 82302175), the STI 2030-Major Projects (grant number 2022ZD0208500), the Key-Area Research and Development Program of Guangdong Province (grant number 2023B0303-030002), the National Science and Technology Innovation 2030 Program (grant number 2021ZD0200500), and the Beijing Nova Program (grant number 20230484465).
Author contributions: G.Y., Z.H., and T.Y. designed the study. Z.H., F.Z., and G.Y. analyzed the data. Z.H. wrote the first draft

of the manuscript. G.Y., Z.H., K.W., T.L., W.L., Y.M., and T.Y. edited the manuscript.
Competing interests: The authors declare that they have no competing interests.

Data Availability

The raw and preprocessed data are available from the HCP (https://www.humanconnectome.org/study/hcp-young-adult/document/1200-subjects-data-release; https://humanconnectome.org/study/hcp-lifespan-development). Human gene expression data are available from the Allen Brain Atlas (https://human.brain-map.org). In our analyses, we also utilized publicly available cortical atlases, including the Schaefer400 atlas (https://github.com/ThomasYeoLab/CBIG/tree/master/stable_projects/brain_parcellation/Schaefer2018_LocalGlobal/Parcellations), the S–A axis (https://github.com/PennLINC/S-A_ArchetypalAxis), and environmental effect maps (https://doi.org/10.5281/zenodo.7606653). The subject lists for both the HCP-YA and HCP-D datasets, along with all predictive feature matrices, are available on our GitHub page (https://github.com/TianyiYanLab/Ethnicity_Race_Diversity). The PLS1 gene lists and *Z* score weights for both cohorts are provided in Data S1. All data supporting the findings of this study are included in the paper and its Supplementary Materials, and all additional information is available from the authors upon reasonable request. All the codes used to generate the results are available on GitHub (https://github.com/TianyiYanLab/Ethnicity_Race_Diversity).

Supplementary Materials

Figs. S1 to S15
Tables S1 to S10

References

1. Kopal J, Uddin LQ, Bzdok D. The end game: Respecting major sources of population diversity. *Nat Methods*. 2023;20(8):1122–1128.
2. Ricard J, Parker T, Dhamala E, Kwasa J, Allsop A, Holmes A. Confronting racially exclusionary practices in the acquisition and analyses of neuroimaging data. *Nat Neurosci*. 2023;26(1):4–11.
3. Harnett NG, Merrill LC, Fani N. Racial and ethnic socioenvironmental inequity and neuroimaging in psychiatry: A brief review of the past and recommendations for the future. *Neuropsychopharmacology*. 2024;50(1):3–15.
4. Dhamala E, Ricard JA, Uddin LQ, Galea LA, Jacobs EG, Yip SW, Yeo BTT, Chakravarty MM, Holmes AJ. Considering the interconnected nature of social identities in neuroimaging research. *Nat Neurosci*. 2024;28:222–233.
5. Harnett NG, Fani N, Rowland G, Kumar P, Rutherford S, Nickerson LD. Population-level normative models reveal race-and socioeconomic-related variability in cortical thickness of threat neurocircuitry. *Commun Biol*. 2024;7(1):745.
6. Yang G, Bozek J, Han M, Gao JH. Constructing and evaluating a cortical surface atlas and analyzing cortical sex differences in young Chinese adults. *Hum Brain Mapp*. 2020;41(9):2495–2513.
7. Dumornay NM, Lebois LA, Ressler KJ, Harnett NG. Racial disparities in adversity during childhood and the false appearance of race-related differences in brain structure. *Am J Psychiatry*. 2023;180(2):127–138.
8. Yang G, Zhou S, Bozek J, Dong H-M, Han M, Zuo X-N, Liu H, Gao JH. Sample sizes and population differences in brain template construction. *NeuroImage*. 2020;206: Article 116318.
9. Fields C, Rosenblatt M, Scheinost D. Racialized heteroscedasticity in connectome-based predictions of brain-behavior relationships. PsyArXiv. 2024. https://doi.org/10.31234/osf.io/yqehw
10. Harnett NG, Fani N, Carter S, Sanchez LD, Rowland GE, Davie WM, Guzman C, Lebois LAM, Ely TD, van Rooij S, et al. Structural inequities contribute to racial/ethnic differences in neurophysiological tone, but not threat reactivity, after trauma exposure. *Mol Psychiatry*. 2023;28(7):2975–2984.
11. Ge J, Yang G, Han M, Zhou S, Men W, Qin L, Lyu B, Li H, Wang H, Rao H, et al. Increasing diversity in connectomics with the Chinese human connectome project. *Nat Neurosci*. 2023;26(1):163–172.
12. Yang G, Bozek J, Noble S, Han M, Wu X, Xue M, Kang J, Jia T, Fu J, Ge J, et al. Global diversity in individualized cortical network topography. *Cereb Cortex*. 2023;33(11):6803–6817.
13. Pang JC, Aquino KM, Oldehinkel M, Robinson PA, Fulcher BD, Breakspear M, Fornito A. Geometric constraints on human brain function. *Nature*. 2023;618(7965):566–574.
14. Fotiadis P, Parkes L, Davis KA, Satterthwaite TD, Shinohara RT, Bassett DS. Structure–function coupling in macroscale human brain networks. *Nat Rev Neurosci*. 2024;25(10):688–704.
15. Seidlitz J, Váša F, Shinn M, Romero-Garcia R, Whitaker KJ, Vértes PE, Wagstyl K, Kirkpatrick Reardon P, Clasen L, Liu S, et al. Morphometric similarity networks detect microscale cortical organization and predict inter-individual cognitive variation. *Neuron*. 2018;97(1):231–247.e37.
16. Cardenas-Iniguez C, Gonzalez MR. Recommendations for the responsible use and communication of race and ethnicity in neuroimaging research. *Nat Neurosci*. 2024;27(4):615–628.
17. Puka K, Kilian C, Zhu Y, Mulia N, Buckley C, Lasserre AM, Rehm J, Probst C. Can lifestyle factors explain racial and ethnic inequalities in all-cause mortality among US adults? *BMC Public Health*. 2023;23(1):1591.
18. Han S, Northoff G. Culture-sensitive neural substrates of human cognition: A transcultural neuroimaging approach. *Nat Rev Neurosci*. 2008;9(8):646–654.
19. Williams DR, Collins C. US socioeconomic and racial differences in health: Patterns and explanations. *Annu Rev Sociol*. 1995;21(1):349–386.
20. Sudano JJ, Baker DW. Explaining US racial/ethnic disparities in health declines and mortality in late middle age: The roles of socioeconomic status, health behaviors, and health insurance. *Soc Sci Med*. 2006;62(4):909–922.
21. Roberts AL, Gilman SE, Breslau J, Breslau N, Koenen KC. Race/ethnic differences in exposure to traumatic events, development of post-traumatic stress disorder, and treatment-seeking for post-traumatic stress disorder in the United States. *Psychol Med*. 2011;41(1):71–83.
22. Noble KG, Houston SM, Brito NH, Bartsch H, Kan E, Kuperman JM, Akshoomoff N, Amaral DG, Bloss CS, Libiger O, et al. Family income, parental education and brain structure in children and adolescents. *Nat Neurosci*. 2015;18(5):773–778.

23. Tomalski P, Moore DG, Ribeiro H, Axelsson EL, Murphy E, Karmiloff-Smith A, Johnson MH, Kushnerenko E. Socioeconomic status and functional brain development–associations in early infancy. *Dev Sci*. 2013;16(5):676–687.
24. Carter SE, Ong ML, Simons RL, Gibbons FX, Lei MK, Beach SR. The effect of early discrimination on accelerated aging among African Americans. *Health Psychol*. 2019;38(11):1010.
25. Fani N, Carter SE, Harnett NG, Ressler KJ, Bradley B. Association of racial discrimination with neural response to threat in black women in the US exposed to trauma. *JAMA Psychiatry*. 2021;78(9):1005–1012.
26. Firth J, Solmi M, Wootton RE, Vancampfort D, Schuch FB, Hoare E, Gilbody S, Torous J, Teasdale SB, Jackson SE, et al. A meta-review of "lifestyle psychiatry": The role of exercise, smoking, diet and sleep in the prevention and treatment of mental disorders. *World Psychiatry*. 2020;19(3):360–380.
27. GBD 2019 Risk Factors Collaborators. Global burden of 87 risk factors in 204 countries and territories, 1990–2019: A systematic analysis for the Global Burden of Disease Study 2019. *Lancet*. 2020;396(10258):1223–1249.
28. Hibar DP, Stein JL, Renteria ME, Arias-Vasquez A, Desrivières S, Jahanshad N, Toro R, Wittfeld K, Abramovic L, Andersson M, et al. Common genetic variants influence human subcortical brain structures. *Nature*. 2015;520(7546):224–229.
29. Richiardi J, Altmann A, Milazzo A-C, Chang C, Chakravarty MM, Banaschewski T, Barker GJ, Bokde AL, Bromberg U, Büchel C, et al. Correlated gene expression supports synchronous activity in brain networks. *Science*. 2015;348(6240):1241–1244.
30. Feng G, Wang Y, Huang W, Chen H, Cheng J, Shu N. Spatial and temporal pattern of structure–function coupling of human brain connectome with development. *eLife*. 2024;13:RP93325.
31. Zhang X-H, Anderson KM, Dong H-M, Chopra S, Dhamala E, Emani PS, Gerstein MB, Margulies DS, Holmes AJ. The cell-type underpinnings of the human functional cortical connectome. *Nat Neurosci*. 2024;28(1):150–160.
32. Morgan SE, Seidlitz J, Whitaker KJ, Romero-Garcia R, Clifton NE, Scarpazza C, van Amelsvoort T, Marcelis M, van Os J, Donohoe G, et al. Cortical patterning of abnormal morphometric similarity in psychosis is associated with brain expression of schizophrenia-related genes. *Proc Natl Acad Sci USA*. 2019;116(19):9604–9609.
33. Li J, Seidlitz J, Suckling J, Fan F, Ji G-J, Meng Y, Yang S, Wang K, Qiu J, Chen H, et al. Cortical structural differences in major depressive disorder correlate with cell type-specific transcriptional signatures. *Nat Commun*. 2021;12(1):1647.
34. Benjamin KJ, Chen Q, Eagles NJ, Huuki-Myers LA, Collado-Torres L, Stolz JM, Pertea G, Shin JH, Paquaola ACM, Hyde TM. Analysis of gene expression in the postmortem brain of neurotypical Black Americans reveals contributions of genetic ancestry. *Nat Neurosci*. 2024;27:1067–1074.
35. Foley KG, Adli M, Kim JJ. Single-nuclei sequencing of uterine serous carcinoma reveals racial differences in immune signaling. *Proc Natl Acad Sci USA*. 2024;121(34):Article e2402998121.
36. Association Association. 2010 Alzheimer's disease facts and figures. *Alzheimers Dement*. 2010;6(2):158–194.
37. Power MC, Bennett EE, Turner RW, Dowling NM, Ciarleglio A, Glymour MM, Gianattasio KZ. Trends in relative incidence and prevalence of dementia across non-Hispanic Black and White individuals in the United States, 2000-2016. *JAMA Neurol*. 2021;78(3):275–284.
38. KESSLER II. Epidemiologic studies of Parkinson's disease: II. A hospital-based survey. *Am J Epidemiol*. 1972;95(4):308–318.
39. Li J, Bzdok D, Chen J, Tam A, Ooi LQR, Holmes AJ, Ge T, Patil KR, Jabbi M, Eickhoff SB, et al. Cross-ethnicity/race generalization failure of behavioral prediction from resting-state functional connectivity. *Sci Adv*. 2022;8(11):Article eabj1812.
40. Kong R, Yang Q, Gordon E, Xue A, Yan X, Orban C, Zuo XN, Spreng N, Ge T, Holmes A, et al. Individual-specific areal-level parcellations improve functional connectivity prediction of behavior. *Cereb Cortex*. 2021;31(10):4477–4500.
41. Schaefer A, Kong R, Gordon EM, Laumann TO, Zuo X-N, Holmes AJ, Eickhoff SB, Yeo BTT. Local-global parcellation of the human cerebral cortex from intrinsic functional connectivity MRI. *Cereb Cortex*. 2018;28(9):3095–3114.
42. Wang D, Buckner RL, Fox MD, Holt DJ, Holmes AJ, Stoecklein S, Langs G, Pan R, Qian T, Li K, et al. Parcellating cortical functional networks in individuals. *Nat Neurosci*. 2015;18(12):1853–1860.
43. Gordon EM, Laumann TO, Gilmore AW, Newbold DJ, Greene DJ, Berg JJ, Ortega M, Hoyt-Drazen C, Gratton C, Sun H, et al. Precision functional mapping of individual human brains. *Neuron*. 2017;95(4):791–807 e797.
44. Fan L, Li H, Zhuo J, Zhang Y, Wang J, Chen L, Yang Z, Chu C, Xie S, Laird AR, et al. The human brainnetome atlas: A new brain atlas based on connectional architecture. *Cereb Cortex*. 2016;26(8):3508–3526.
45. Chen J, Tam A, Kebets V, Orban C, Ooi LQR, Asplund CL, Marek S, Dosenbach NUF, Eickhoff SB, Bzdok D, et al. Shared and unique brain network features predict cognitive, personality, and mental health scores in the ABCD study. *Nat Commun*. 2022;13(1):1–17.
46. Haufe S, Meinecke F, Görgen K, Dähne S, Haynes J-D, Blankertz B, Bießmann F. On the interpretation of weight vectors of linear models in multivariate neuroimaging. *NeuroImage*. 2014;87:96–110.
47. Sydnor VJ, Larsen B, Seidlitz J, Adebimpe A, Alexander-Bloch AF, Bassett DS, Bertolero MA, Cieslak M, Covitz S, Fan Y, et al. Intrinsic activity development unfolds along a sensorimotor–association cortical axis in youth. *Nat Neurosci*. 2023;26(4):638–649.
48. Yang S, Wagstyl K, Meng Y, Zhao X, Li J, Zhong P, Li B, Fan YS, Chen H, Liao W. Cortical patterning of morphometric similarity gradient reveals diverged hierarchical organization in sensory-motor cortices. *Cell Rep*. 2021;36(8):Article 109582.
49. Fields RD. White matter in learning, cognition and psychiatric disorders. *Trends Neurosci*. 2008;31(7):361–370.
50. Glasser MF, Van Essen DC. Mapping human cortical areas in vivo based on myelin content as revealed by T1-and T2-weighted MRI. *J Neurosci*. 2011;31(32):11597–11616.
51. Soldan A, Pettigrew C, Zhu Y, Wang M-C, Bilgel M, Hou X, Lu H, Miller MI, Albert M, BIOCARD Research Team. Association of lifestyle activities with functional brain connectivity and relationship to cognitive decline among older adults. *Cereb Cortex*. 2021;31(12):5637–5651.
52. Rolls ET, Feng R, Feng J. Lifestyle risks associated with brain functional connectivity and structure. *Hum Brain Mapp*. 2023;44(6):2479–2492.

53. Zhao Y, Yang L, Sahakian BJ, Langley C, Zhang W, Kuo K, Li Z, Gan Y, Li Y, Zhao Y, et al. The brain structure, immunometabolic and genetic mechanisms underlying the association between lifestyle and depression. *Nat Ment Health*. 2023;1(10):736–750.
54. Tian YE, Cole JH, Bullmore ET, Zalesky A. Brain, lifestyle and environmental pathways linking physical and mental health. *Nat Ment Health*. 2024;2:1250–1261.
55. Xue K, Gao B, Chen F, Wang M, Cheng J, Zhang B, Zhu W, Qiu S, Geng Z, Zhang X, et al. Covariation of preadult environmental exposures, adult brain imaging phenotypes, and adult personality traits. *Mol Psychiatry*. 2023;28(11):4853–4866.
56. Liu F, Xu J, Guo L, Qin W, Liang M, Schumann G, Yu C. Environmental neuroscience linking exposome to brain structure and function underlying cognition and behavior. *Mol Psychiatry*. 2023;28(1):17–27.
57. Sydnor VJ, Larsen B, Bassett DS, Alexander-Bloch A, Fair DA, Liston C, Mackey AP, Milham MP, Pines A, Roalf DR, et al. Neurodevelopment of the association cortices: Patterns, mechanisms, and implications for psychopathology. *Neuron*. 2021;109(18):2820–2846.
58. Hawrylycz MJ, Lein ES, Guillozet-Bongaarts AL, Shen EH, Ng L, Miller JA, van de Lagemaat L, Smith KA, Ebbert A, Riley ZL, et al. An anatomically comprehensive atlas of the adult human brain transcriptome. *Nature*. 2012;489(7416):391–399.
59. Sunkin SM, Ng L, Lau C, Dolbeare T, Gilbert TL, Thompson CL, Hawrylycz M, Dang C. Allen Brain Atlas: An integrated spatio-temporal portal for exploring the central nervous system. *Nucleic Acids Res*. 2012;41(D1):D996–D1008.
60. Abdi H. Partial least squares regression and projection on latent structure regression (PLS regression). *Wiley Interdisc Rev Comput Stat*. 2010;2(1):97–106.
61. Yeung C-YC, Taylor SH, Garva R, Holmes DF, Zeef LA, Soininen R, Boot-Handford RP, Kadler KE. Arhgap28 is a RhoGAP that inactivates RhoA and downregulates stress fibers. *PLOS ONE*. 2014;9(9):Article e107036.
62. Tcherkezian J, Lamarche-Vane N. Current knowledge of the large RhoGAP family of proteins. *Biol Cell*. 2007;99(2):67–86.
63. Stephens HA. MICA and MICB genes: Can the enigma of their polymorphism be resolved? *Trends Immunol*. 2001;22(7):378–385.
64. Zhou Y, Zhou B, Pache L, Chang M, Khodabakhshi AH, Tanaseichuk O, Benner C, Chanda SK. Metascape provides a biologist-oriented resource for the analysis of systems-level datasets. *Nat Commun*. 2019;10(1):1523.
65. Bijsterbosch JD, Woolrich MW, Glasser MF, Robinson EC, Beckmann CF, Van Essen DC, Harisson SJ, Smith SM. The relationship between spatial configuration and functional connectivity of brain regions. *eLife*. 2018;7:Article e32992.
66. Cui Z, Li H, Xia CH, Larsen B, Adebimpe A, Baum GL, Cieslak M, Gur RE, Gur RC, Moore TM, et al. Individual variation in functional topography of association networks in youth. *Neuron*. 2020;106(2):340–353.e348.
67. Shanmugan S, Seidlitz J, Cui Z, Adebimpe A, Bassett DS, Bertolero MA, Davatzikos C, Fair DA, Gur RE, Gur RC, et al. Sex differences in the functional topography of association networks in youth. *Proc Natl Acad Sci USA*. 2022;119(33):Article e2110416119.
68. Valk SL, Xu T, Paquola C, Park B-y, Bethlehem RA, Vos de Wael R, Royer J, Masouleh SK, Bayrak Ş, Kochunov P, et al. Genetic and phylogenetic uncoupling of structure and function in human transmodal cortex. *Nat Commun*. 2022;13(1):2341.
69. Sebenius I, Dorfschmidt L, Seidlitz J, Alexander-Bloch A, Morgan SE, Bullmore E. Structural MRI of brain similarity networks. *Nat Rev Neurosci*. 2024;26(1):42–59.
70. Keller AS, Moore TM, Luo A, Visoki E, Gataviņš MM, Shetty A, Cui Z, Fan Y, Ferczko E, Houghton A, et al. A general exposome factor explains individual differences in functional brain network topography and cognition in youth. *Dev Cogn Neurosci*. 2024;66:Article 101370.
71. Poldrack RA. Can cognitive processes be inferred from neuroimaging data? *Trends Cogn Sci*. 2006;10(2):59–63.
72. Kao G, Thompson JS. Racial and ethnic stratification in educational achievement and attainment. *Annu Rev Sociol*. 2003;29(1):417–442.
73. Espinosa LL, Turk JM, Taylor M, Chessman HM. *Race and ethnicity in higher education: A status report*. Washington (DC): American Council on Education; 2019.
74. Ali MM, Creedon T, Bagalman E, Bui J, Clemans-Cope L, Winiski E, Ramos C, Taylor KJ, Allen EH. *Substance use and substance use disorders by race and ethnicity, 2015-2019*. Washington (DC): U.S. Department of Health and Human Services; 2023.
75. Gordon EM, Lynch CJ, Gratton C, Laumann TO, Gilmore AW, Greene DJ, Ortega M, Nguyen AL, Schlaggar BL, Petersen SE, et al. Three distinct sets of connector hubs integrate human brain function. *Cell Rep*. 2018;24(7):1687–1695.e84.
76. Kim P, Evans GW, Angstadt M, Ho SS, Sripada CS, Swain JE, Liberzon I, Phan KL. Effects of childhood poverty and chronic stress on emotion regulatory brain function in adulthood. *Proc Natl Acad Sci USA*. 2013;110(46):18442–18447.
77. Goodman AM, Harnett NG, Knight DC. Pavlovian conditioned diminution of the neurobehavioral response to threat. *Neurosci Biobehav Rev*. 2018;84:218–224.
78. Zhang Z, Zhao Q, Xu J, Yang K, Wu Y, Lei M, Wu Q, Wang H, Cai W, An Q, et al. Linking environmental exposures to depression: Insights from epidemiology, biology, and methodology. *Brain Conflux*. 2025;1(2):e244.
79. Stern Y. What is cognitive reserve? Theory and research application of the reserve concept. *J Int Neuropsychol Soc*. 2002;8(3):448–460.
80. Barulli DJ, Rakitin BC, Lemaire P, Stern Y. The influence of cognitive reserve on strategy selection in normal aging. *J Int Neuropsychol Soc*. 2013;19(7):841–844.
81. Barulli D, Stern Y. Efficiency, capacity, compensation, maintenance, plasticity: Emerging concepts in cognitive reserve. *Trends Cogn Sci*. 2013;17(10):502–509.
82. Bozzali M, Dowling C, Serra L, Spanò B, Torso M, Marra C, Castelli D, Dowell NG, Koch G, Caltagirone C, et al. The impact of cognitive reserve on brain functional connectivity in Alzheimer's disease. *J Alzheimer's Dis*. 2015;44(1):243–250.
83. Seyedsalehi A, Warrier V, Bethlehem RA, Perry BI, Burgess S, Murray GK. Educational attainment, structural brain reserve and Alzheimer's disease: A Mendelian randomization analysis. *Brain*. 2023;146(5):2059–2074.
84. Volkow ND, Wang G-J, Fowler JS, Tomasi D, Telang F. Addiction: Beyond dopamine reward circuitry. *Proc Natl Acad Sci USA*. 2011;108(37):15037–15042.
85. Singleton SP, Velidi P, Schilling L, Luppi AI, Jamison K, Parkes L, Kuceyeski A. Altered structural connectivity and

functional brain dynamics in individuals with heavy alcohol use elucidated via network control theory. *Biol Psychiatry Cogn Neurosci Neuroimaging*. 2024;9(10):1010–1018.
86. Li C-sR, Sinha R. Inhibitory control and emotional stress regulation: Neuroimaging evidence for frontal–limbic dysfunction in psycho-stimulant addiction. *Neurosci Biobehav Rev*. 2008;32(3):581–597.
87. Tidey JW, Miller ME. Smoking cessation and reduction in people with chronic mental illness. *BMJ*. 2015;351: Article h4065.
88. Xiang S, Jia T, Xie C, Cheng W, Chaarani B, Banaschewski T, Barker GJ, Bokde ALW, Büchel C, Desrivières S, et al. Association between vmPFC gray matter volume and smoking initiation in adolescents. *Nat Commun*. 2023;14(1):4684.
89. Shokri-Kojori E, Tomasi D, Wiers CE, Wang G-J, Volkow ND. Alcohol affects brain functional connectivity and its coupling with behavior: Greater effects in male heavy drinkers. *Mol Psychiatry*. 2017;22(8):1185–1195.
90. MacKillop J, Agabio R, Feldstein Ewing SW, Heilig M, Kelly JF, Leggio L, Lingford-Hughes A, Palmer AA, Parry CD, Ray L, et al. Hazardous drinking and alcohol use disorders. *Nat Rev Dis Primers*. 2022;8(1):80.
91. Cohen S, Greenberg ME. Communication between the synapse and the nucleus in neuronal development, plasticity, and disease. *Annu Rev Cell Dev Biol*. 2008;24(1):183–209.
92. Preller KH, Burt JB, Ji JL, Schleifer CH, Adkinson BD, Stämpfli P, Seifritz E, Repovs G, Krystal JH, Murray JD, et al. Changes in global and thalamic brain connectivity in LSD-induced altered states of consciousness are attributable to the 5-HT2A receptor. *eLife*. 2018;7:Article e35082.
93. Wang X-J. Macroscopic gradients of synaptic excitation and inhibition in the neocortex. *Nat Rev Neurosci*. 2020;21(3):169–178.
94. Tau GZ, Peterson BS. Normal development of brain circuits. *Neuropsychopharmacology*. 2010;35(1):147–168.
95. Jiang X, Nardelli J. Cellular and molecular introduction to brain development. *Neurobiol Dis*. 2016;92:3–17.
96. Liang X, Sun L, Liao X, Lei T, Xia M, Duan D, Zeng Z, Li Q, Xu Z, Men W, et al. Structural connectome architecture shapes the maturation of cortical morphology from childhood to adolescence. *Nat Commun*. 2024;15(1):784.
97. Stringhini S, Polidoro S, Sacerdote C, Kelly RS, Van Veldhoven K, Agnoli C, Grioni S, Tumino R, Giurdanella MC, Panico S, et al. Life-course socioeconomic status and DNA methylation of genes regulating inflammation. *Int J Epidemiol*. 2015;44(4):1320–1330.
98. Kapoor M, Wang J-C, Farris SP, Liu Y, McClintick J, Gupta I, Meyers JL, Bertelsen S, Chao M, Nurnberger J, et al. Analysis of whole genome-transcriptomic organization in brain to identify genes associated with alcoholism. *Transl Psychiatry*. 2019;9(1):89.
99. Rahman MF, McGowan PO. Cell-type-specific epigenetic effects of early life stress on the brain. *Transl Psychiatry*. 2022;12(1):326.
100. Grazioli E, Dimauro I, Mercatelli N, Wang G, Pitsiladis Y, Di Luigi L, Caporossi D. Physical activity in the prevention of human diseases: Role of epigenetic modifications. *BMC Genomics*. 2017;18:111–123.
101. Vetr NG, Gay NR, Montgomery SB. The impact of exercise on gene regulation in association with complex trait genetics. *Nat Commun*. 2024;15(1):3346.
102. Han Z, Yang G, Liu T, Funahashi S, Zuo X-N, Yan T. Enriching population diversity in neuroscience. *Sci Bull*. 2025;79(16):2560–2564.
103. Sebenius I, Seidlitz J, Warrier V, Bethlehem RA, Alexander-Bloch A, Mallard TT, Garcia RR, Bullmore ET, Morgan SE. Robust estimation of cortical similarity networks from brain MRI. *Nat Neurosci*. 2023;26(8):1461–1471.
104. Liang X, Sun L, Xia M, Zhao T, Gong G, Li Q, Liao X, Cui Z, Duan D, Pang C, et al. Dissecting human cortical similarity networks across the lifespan. *Neuron*. 2025;113(19):3275–3295.e3211.
105. Sun L, Zhao T, Liang X, Xia M, Li Q, Liao X, Gong G, Wang Q, Pang C, Yu Q, et al. Human lifespan changes in the brain's functional connectome. *Nat Neurosci*. 2025;28(4):891–901.
106. Ryali S, Zhang Y, de Los C, Supekar K, Menon V. Deep learning models reveal replicable, generalizable, and behaviorally relevant sex differences in human functional brain organization. *Proc Natl Acad Sci USA*. 2024;121(9):Article e2310012121.
107. Van Essen DC, Smith SM, Barch DM, Behrens TE, Yacoub E, Ugurbil K, WU-Minn HCP Consortium. The WU-Minn human connectome project: An overview. *NeuroImage*. 2013;80:62–79.
108. Harms MP, Somerville LH, Ances BM, Andersson J, Barch DM, Bastiani M, Bookheimer SY, Brown TB, Buckner RL, Burgess GC, et al. Extending the human connectome project across ages: Imaging protocols for the lifespan development and aging projects. *NeuroImage*. 2018;183:972–984.
109. Glasser MF, Sotiropoulos SN, Wilson JA, Coalson TS, Fischl B, Andersson JL, Xu J, Jbabdi S, Webster M, Polimeni JR, et al. The minimal preprocessing pipelines for the Human Connectome Project. *NeuroImage*. 2013;80:105–124.
110. Dhamala E, Ooi LQR, Chen J, Ricard JA, Berkeley E, Chopra S, Qu Y, Zhang XH, Lawhead C, Yeo BTT, et al. Brain-based predictions of psychiatric illness–linked behaviors across the sexes. *Biol Psychiatry*. 2023;94(6):479–491.
111. Serio B, Hettwer MD, Wiersch L, Bignardi G, Sacher J, Weis S, Eickhoff SB, Valk SL. Sex differences in functional cortical organization reflect differences in network topology rather than cortical morphometry. *Nat Commun*. 2024;15(1):7714.
112. Markello RD, Arnatkeviciute A, Poline J-B, Fulcher BD, Fornito A, Misic B. Standardizing workflows in imaging transcriptomics with the abagen toolbox. *eLife*. 2021;10:Article e72129.
113. Fulcher BD, Arnatkeviciute A, Fornito A. Overcoming false-positive gene-category enrichment in the analysis of spatially resolved transcriptomic brain atlas data. *Nat Commun*. 2021;12(1):2669.
114. Vos de Wael R, Benkarim O, Paquola C, Lariviere S, Royer J, Tavakol S, Xu T, Hong SJ, Langs G, Valk S, et al. BrainSpace: A toolbox for the analysis of macroscale gradients in neuroimaging and connectomics datasets. *Commun Biol*. 2020;3(1):103.
115. Mowinckel AM, Vidal-Piñeiro D. Visualization of brain statistics with R packages ggseg and ggseg3d. *Adv Methods Pract Psychol Sci*. 2020;3(4):466–483.